Clim Dyn (2012) 38:1167–1180
DOI 10.1007/s00382-011-1237-4

Impact of MJO on the diurnal cycle of rainfall over the western Maritime Continent in the austral summer

Ji-Hyun Oh · Kwang-Yul Kim · Gyu-Ho Lim

Received: 5 October 2010 / Accepted: 28 October 2011 / Published online: 12 November 2011

Abstract This paper investigates the impact of the Madden-Julian Oscillation (MJO) on the diurnal cycle of rainfall over the western Maritime Continent during the austral summer. For this purpose, cyclostationary empirical orthogonal function analysis is applied to the tropical rainfall measuring mission rain rate and the Japanese Reanalysis-25 data for the period 1998–2008. The real-time multivariate MJO index by Wheeler and Hendon (Mon Wea Rev 132:1917–1932, 2004) is adopted to define the intensity and the phase of MJO. It is demonstrated that the hourly maximum rain rate over the domain tends to increase when convectively active phase of MJO approaches the Maritime Continent. In contrast, the hourly maximum rain rate tends to decrease when convectively suppressed phase of MJO resides over the region. The changes in the rain rate due to MJO differ over the ocean and the land. This difference is the greatest when the MJO is in the mature stage. Throughout the day during this stage, terrestrial rain rates show minimum values while diurnally varying oceanic rain rates record maximum values. Thus, precipitation becomes more intense in the morning over the Java Sea and is weakened in the evening over Borneo and Sumatra during the mature stage of MJO. During the decaying stage of MJO over the Maritime Continent, the diurnal cycle of precipitation weakens significantly over the ocean but only weakly over land. Analyses suggest that the anomalous lower level winds accompanied by MJO interact with the monsoonal flow over the Maritime Continent. Westerlies induced by MJO convection in the mature stage are superimposed on the monsoonal westerlies over the equator and increase wind speed mainly over the Java Sea due to the blocking effect of orography. Mountainous islands induce flow bifurcation, causing near-surface winds to converge mainly over the oceanic channels between two islands. As a result, heat flux release from the ocean to the atmosphere is enhanced by the increased surface wind resulting in instability as described in the wind-induced surface heat exchange mechanism. This may contribute to heavy rainfall over the Java Sea in the morning during the mature stage. On the other hand, convergence and vertical velocity over the islands, which play important roles in inducing nighttime rainfall, tend to be weak in the evening during the mature stage of MJO. Strong westerlies arising from MJO and the seasonal flow during the mature stage tend to interrupt convergence over islands. This interruption of convergence by MJO gives rise to decreased rain rates over the land regions.

Keywords Diurnal cycle · MJO · Maritime Continent · CSEOF

1 Introduction

The Maritime Continent includes a complex network of islands and seas. This region has a prominent diurnal cycle of rainfall that exhibits a distinct land-sea contrast (Ichikawa and Yasunari 2006; Qian 2008). While a maximum amount of rainfall occurs in the late afternoon/evening over land, precipitation over the oceanic regions reaches its maximum at night/early morning (Yang and Slingo 2001; Ichikawa and Yasunari 2006; Zhou and Wang 2006; Qian 2008).

Since Madden-Julian Oscillations (MJOs) with periodicities of ~30–60 days were observed for various

J.-H. Oh · K.-Y. Kim · G.-H. Lim (✉)
School of Earth and Environmental Sciences, Seoul National University, Seoul 151-742, Korea
e-mail: gyuholim@snu.ac.kr

meteorological variables, numerous observational and modeling studies have been conducted to study their initiation, propagation, and general characteristics (Rui and Wang 1990; Hendon and Salby 1994; Slingo et al. 1996; Sperber 2003). Austral summer MJO develops over the Indian Ocean and propagates eastward along the equator passing over the Maritime Continent. According to previous studies, the Maritime Continent tends to weaken MJO convection (Seo and Kim 2003; Hsu and Lee 2005; Wu and Hsu 2009). A convectively enhanced phase of MJO was observed to shift suddenly from one region to another over the Maritime Continent (Ichikawa and Yasunari 2007). After its steady propagation is disturbed by the Maritime Continent, MJO rejuvenates and keeps on moving eastward during the austral summer.

Earlier studies revealed that MJO is closely tied to atmospheric phenomena on various temporal and spatial scales such as the Asian/Australian monsoons (Sui and Lau 1992; Lawrence and Webster 2002; Hendon and Liebmann 1990), tropical cyclones (Maloney and Hartmann 2000; Hall et al. 2001) and El Niño-Southern Oscillation (ENSO) (Kessler and Kleeman 2000; Zhang and Gottschalck 2002). Similarly, MJO may affect the diurnal cycle of precipitation over the Maritime Continent and may also be influenced by the diurnal cycle. In this paper, investigation will be made on the impact that the passage of MJO exerts on the diurnal cycle of rainfall over the Maritime Continent. Since the Maritime Continent is a major atmospheric heat source releasing significant amount of latent heat (Dayem et al. 2007), regional precipitation process plays an important role not only for the regional climate predictability but also for the global climate sensitivity and predictability.

Numerous studies have focused on the scale interaction between MJO and the diurnal cycle of rainfall (Sui and Lau 1992; Chen and Houze 1997; Tian et al. 2006; Ichikawa and Yasunari 2008). However, some disparities exist in earlier studies with respect to how the amplitude and the phase of the diurnal cycle are affected by MJO. Further, analysis domains differ for each study and do not necessarily focus on the Maritime Continent. For example, Chen and Houze (1997) investigated the diurnal cycle of tropical deep convection over the western Pacific warm pool region using satellite infrared data and in situ surface measurements from the Tropical Ocean Global Atmosphere Coupled Ocean–Atmosphere Response Experiment (TOGA COARE). They found that cloud systems are spatially small and their lifetimes are relatively short during the convectively suppressed phase of MJO. The systems reach their maximum size in the afternoon and then dissipate. Meanwhile, spatially larger cloud systems form in the afternoon and are longer-lived during the active phase of MJO; they reach their maximum areal extent during night-to-dawn hours and decay after sunrise. Tian et al. (2006) demonstrated that the diurnal cycle of tropical deep convective cloud (DCC) amount is enhanced (reduced) over both the ocean and land during the convectively enhanced (suppressed) phase of MJO. On the other hand, the phase of the diurnal cycle of DCC is rarely affected by MJO over the Indo-Pacific warm pool region including the Indian Ocean. Contrary to the studies above, Sui and Lau (1992) reported an opposite relationship between the diurnal cycle and intraseasonal disturbances over the Maritime Continent; they found that the period of active intraseasonal variability is characterized by a diminished diurnal cycle and vice versa. On the other hand, Ichikawa and Yasunari (2006, 2008) showed that the diurnal cycles of rainfall over Borneo and New Guinea, major islands of the Maritime Continent, are modulated by low-level winds varying on intraseasonal time scales using Tropical Rainfall Measuring Mission (TRMM) precipitation radar data. They found that the dynamical evolution of the diurnal rainfall differs between the active and inactive periods of MJO.

After the launch of the TRMM satellite in 1998, data acquired from the mission were analyzed in an attempt to understand the diurnal cycle over the tropics (Nesbitt and Zipser 2003; Bowman et al. 2005; Yang and Smith 2006; Zhou and Wang 2006; Ichikawa and Yasunari 2007). These studies showed that the diurnal cycle of rainfall over the terrestrial region differs significantly in phase and mechanism from that of the oceanic region (Nesbitt and Zipser 2003; Bowman et al. 2005). It was also noted that the relationship between the diurnal variation of rainfall and large-scale disturbance associated with MJO over the ocean differs from that over land (Ichikawa and Yasunari 2007). Yet, little is known about the disparate impact of MJO on the diurnal cycle over the terrestrial and the oceanic regions of the Maritime Continent. Due to the land-sea contrast of latent heat flux and the orographic effect over land, the diurnal cycle of precipitation and the MJO may interact differently over land than over the ocean.

Although previous studies have been conducted using various analytical techniques and data to reveal the impact of MJO on the diurnal cycle over the Maritime Continent, their results do not agree. This study focuses on this issue, particularly on the MJO's modulation of the diurnal variation of rainfall over the Maritime Continent with specific distinction of the terrestrial and the oceanic regions. In addition, plausible physical explanations for the MJO's modulation of the diurnal cycle are offered. Austral summer period, during which MJO signals are strongest, is chosen for examination in the present study. Statistical analysis called the cyclostationary empirical orthogonal function (CSEOF) technique is used. This method enables us to extract the diurnal cycle from the datasets as well as the temporal variation of its strength.

This paper is outlined as follows. Section 2 describes the datasets used in this study. The method of analysis is presented in Sect. 3. Section 4 examines climatological characteristics of the diurnal cycle over the Maritime Continent and the impact of MJO on the diurnal variation of precipitation. Plausible explanations are proposed for the link between MJO and diurnal variability over the sea and land in Sect. 4. A summary and discussion are provided in Sect. 5.

2 Data

TRMM 3B42 (version 6) rainfall data, which are derived from combination of high quality microwave estimates and variable rain rate IR estimates, were used for the present study (http://trmm.gsfc.nasa.gov/3b42.html). The dataset also make use of TRMM Combined Instrument estimate, which derives from TRMM Microwave Imager and precipitation radar, GPCP monthly rain gauge analysis, and Climate Assessment and Monitoring System monthly rain gauge analysis (Huffman et al. 2007). The dataset covers 50°S to 50°N with a 0.25° longitude-latitude spatial resolution at a 3-h time interval. It was acquired via anonymous ftp from disc2.nascom.nasa.gov. In order to explain the physical and dynamical processes associated with the diurnal cycle of precipitation over the western Maritime Continent during the austral summer (DJF) and the impact of MJO on the diurnal variation of rainfall, Japanese 25-year Reanalysis (JRA-25) provided by the Japan Meteorological Agency and the Central Research Institute of Electric Power Industry (JMA-CRIEPI) were also used. The JRA-25 dataset has a 1.25° × 1.25° horizontal resolution and a 6-h temporal resolution and was acquired from the web site http://jra.kishou.go.jp/JRA-25 (Onogi et al. 2007).

In addition, daily-averaged outgoing long wave radiation (OLR) data from the United States National Oceanic and Atmospheric Administration (NOAA) were used to extract the patterns of eastward propagating MJO. The Real-Time Multivariate MJO (RMM) index derived by Wheeler and Hendon (2004) was acquired from the website of the Bureau of Meteorology Research Centre, Australia (http://www.cawcr.gov.au/bmrc/).

3 Method of analysis

3.1 CSEOF analysis

The datasets described above were analyzed for the 10 austral summers (DJF) from 1998/1999 to 2007/2008. Each winter consists of 90 days. The domain of analysis in the present study is 100°E–125°E × 10°S–5°N; this region covers the western part of the Maritime Continent, which encounters eastward propagating MJOs. Empirical orthogonal function (EOF) analysis was first performed on the TRMM rain rate. Then, CSEOF analysis was conducted in the EOF space with a nested period of 1 day (= eight 3-h intervals) in order to extract the diurnal cycle of the rain rate. The first 100 EOFs were used as basis functions; these 100 EOFs together explain about 50% of the total variability.

In CSEOF analysis (Kim et al. 1996; Kim and North 1997), space–time data $T(r, t)$ are decomposed into

$$T(r,t) = \sum_{n} LV_n(r,t)PC_n(t), \tag{1}$$

where $LV_n(r, t)$ are cyclostationary loading vectors and $PC_n(t)$ are corresponding principal component (PC) time series. The cyclostationary loading vectors are periodic in time:

$$LV_n(r,t) = LV_n(r,t+d), \tag{2}$$

where d is the nested period. Thus, each $LV_n(r, t)$ describes daily and sub-daily physical evolution of rain rate and corresponding PC time series, $PC_n(t)$, describes the variation of the amplitude on time scales longer than 1 day. CSEOF loading vectors, such as $LV_n(r, t)$, are time dependent and periodic because they are derived from a time-dependent and periodic covariance function.

3.2 Regression analysis

After CSEOF analysis is performed separately for individual variables, regression analysis should be conducted in order to make individual variables physically consistent with each other (Seo and Kim 2003). The PC time series of a predictor variable, such as wind, are regressed on the PC time series of precipitation (target variable in this study):

$$PC_n(t) = \sum_{m=1}^{M} \alpha_m^{(n)} PCP_m(t) + \varepsilon^{(n)}(t), \tag{3}$$

where $PC_n(t)$ are the PC time series of the rain rate, $PCP_m(t)$ are the PC time series of a predictor variable, and $\alpha_m^{(n)}$ are regression coefficients. Then, a new loading vector is obtained by

$$LVP_n^{(reg)}(r,t) = \sum_{m=1}^{M} \alpha_m^{(n)} LVP_m(r,t), \tag{4}$$

where $LVP_m(r, t)$ are the loading vectors of the predictor variable and $LVP_n^{(reg)}(r,t)$ denotes the new loading vector of the predictor variable, which is physically consistent with the nth loading vector of the rain rate. As a result of regression analysis, the entire dataset can be written as

$$Data(r,t) = \sum_{n} \{PR_n(r,t), ST_n(r,t), U_n(r,t), V_n(r,t), \ldots\} PC_n(t), \quad (5)$$

where $PR_n(r, t)$ represents the loading vectors of the rain rate (target variable) and $ST_n(r, t)$, $U_n(r, t)$, $V_n(r, t)$, for example, are the regressed loading vectors of surface air temperature, zonal wind, and meridional wind. Although the physical evolutions of individual variables are distinct, their amplitudes are all governed by a single time series, $PC_n(t)$, which is the PC time series of the rain rate (target variable).

3.3 Classification of MJO phases

To examine the impact of MJO on the diurnal cycle of rainfall over the western region of the Maritime Continent, it is necessary to define the dates in which the convection of MJO reaches the western Maritime Continent. These dates were determined by using the RMM index derived by Wheeler and Hendon (2004). The RMM index is constructed by the two leading principal component time series, RMM1 and RMM2, of the EOFs of zonal winds at 850 and 200 hPa. The RMM1 and RMM2 construct the two-dimensional phase space of MJO and represent the location of MJO in phase space as a point (RMM1, RMM2).The distance of a point from the origin determines the amplitude of MJO. The phase space is divided into eight sectors, from which the location of the MJO convective center between Africa and the eastern Pacific can be inferred. We utilized the RMM index for composite analysis. Only the cases with the amplitude of MJO being greater than unity were chosen.

4 Results

4.1 Characteristics of the diurnal cycle of rainfall

The first CSEOF of the TRMM rain rate represents the diurnal cycle of precipitation in the austral summer (DJF) over the western Maritime Continent. The diurnal variation of precipitation and other physical variables are shown in Fig. 1. As mentioned in previous studies, there exists a distinct land–ocean contrast in the phase of the diurnal cycle of rainfall (Yang and Slingo 2001; Ichikawa and Yasunari 2006; Mori et al. 2004).Rainfall over the islands is at its maximum in late afternoon/evening and at its minimum in early morning. Panels a–h in Fig. 1 exhibit that rainfall begins along the coastline and gradually shifts inland (to areas such as Borneo and Sumatra) during 1700–2300 LST. After reaching its maximum over the islands, rainfall shifts offshore during 0200–1100 LST.

Evolution of other atmospheric variables associated with the diurnal cycle of rainfall is shown in Fig. 1i–p. Since the land surface has a lower heat capacity than the ocean surface, temperature variation by solar heating is more significant over land than over the ocean. When the sun rises, temperature over land increases rapidly until the sun reaches its maximum altitude. This causes pressure gradient to increase between the ocean and land and static destabilization of the atmosphere over land (Bowman et al. 2005; Yang and Smith 2006). The daytime sea breeze is induced due to the pressure gradient, resulting in moisture supply by sea breezes together with forced ascent of air. Equivalent potential temperature difference between 850 and 500 hPa indicates conditional instability. Convective instability is enhanced over the islands at 1400 LST. Strong upward motion and lower level convergence prevails over islands, such as Borneo, Sumatra, and Sulawesi at 2000 LST. As a result, late-afternoon and evening precipitation tends to develop over land. The situation reverses after the sunset. Radiative cooling during the night stabilizes the atmospheric column over land and precipitation gradually diminishes until morning.

According to Qian (2008), since mountain-valley breezes are roughly in phase with land-sea breezes over the mountainous coastal region, those may combine to strengthen the diurnal cycle of winds and form extended land-sea breezes. On the other hand, low-level convergence of the prevailing northeasterly monsoonal flow and the land breeze contributes to oceanic precipitation adjacent to the northwest Borneo from midnight until morning (Houze et al. 1981; Ichikawa and Yasunari 2006; Liberti et al. 2001). Similarly, land breezes from adjacent islands converge over the seas between the islands (e.g., between Borneo and southern Sumatra) at night and induce nighttime precipitation (Qian 2008).

4.2 Spatial distribution of MJO based on the RMM index

Composite maps of daily OLR and 850 hPa wind anomalies for individual phases of MJO based on the RMM index are shown in Fig. 2. For composite analysis, only cases in which the amplitude of MJO was greater than unity were chosen; the number of days selected for compositing is given in parentheses for each phase in Fig. 2. The rectangular box in the composite domain denotes the western Maritime Continent. As shown in the figure, eastward propagating MJO is reasonably well captured with respect to the RMM index. MJO convection initiated over the western Indian Ocean in phase 1 moves eastward and approaches the western part of the Maritime Continent near Sumatra, Borneo and the Java Sea in phase 3 (see also Seo and Kim 2003). Prevailing easterly wind anomalies in phase 1 change into westerly

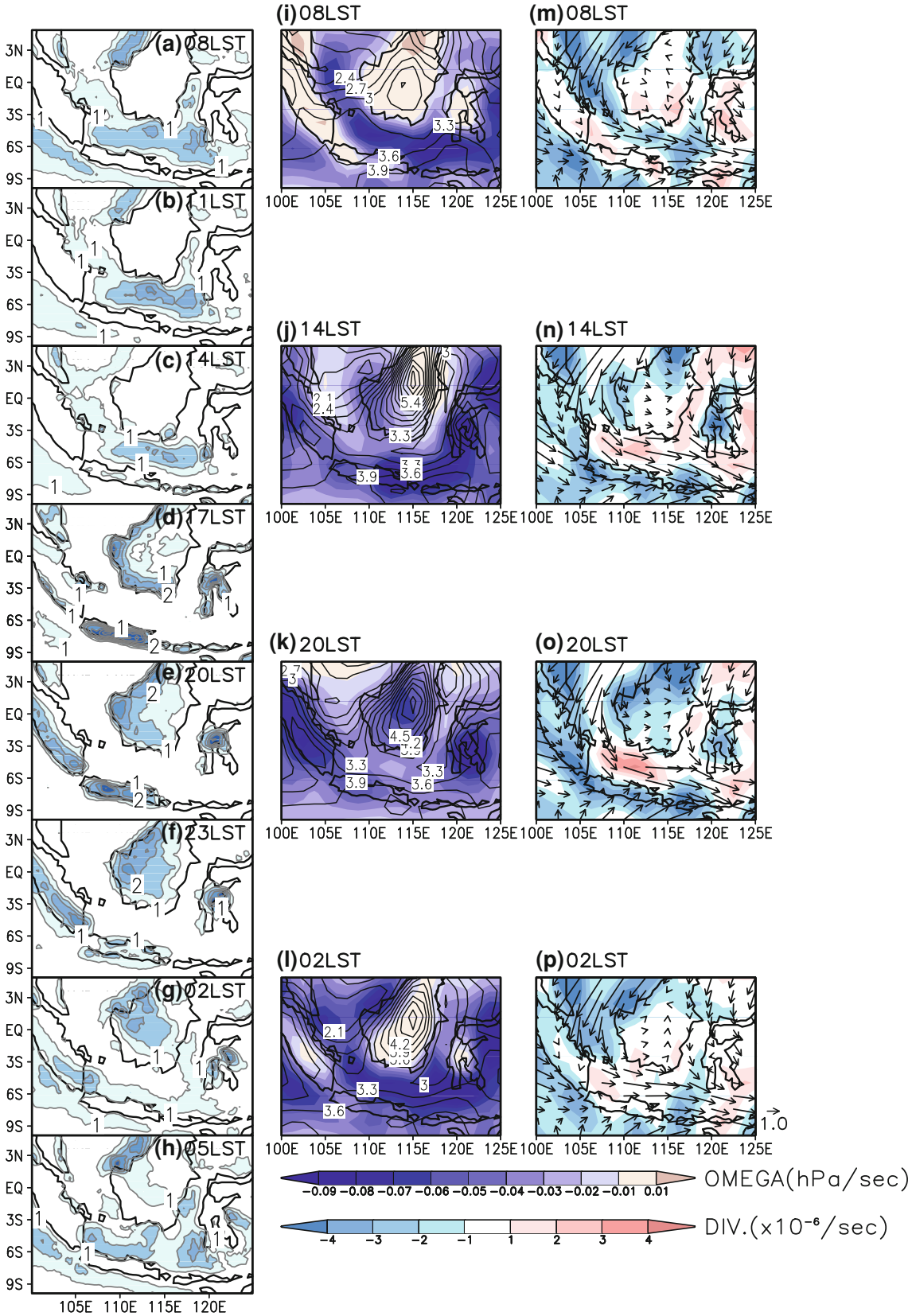

Fig. 1 Evolution of **a–h** TRMM rain rate (mm h^{-1}), **i–l** 500 hPa pressure velocity (shaded, hPa sec^{-1}) and difference of equivalent potential temperatures between 850 hPa and 500 hPa (contoured, °K), and **m–p** 10 m wind (vector, m s^{-1}) and surface divergence (shaded, s^{-1}) in association with the diurnal cycle

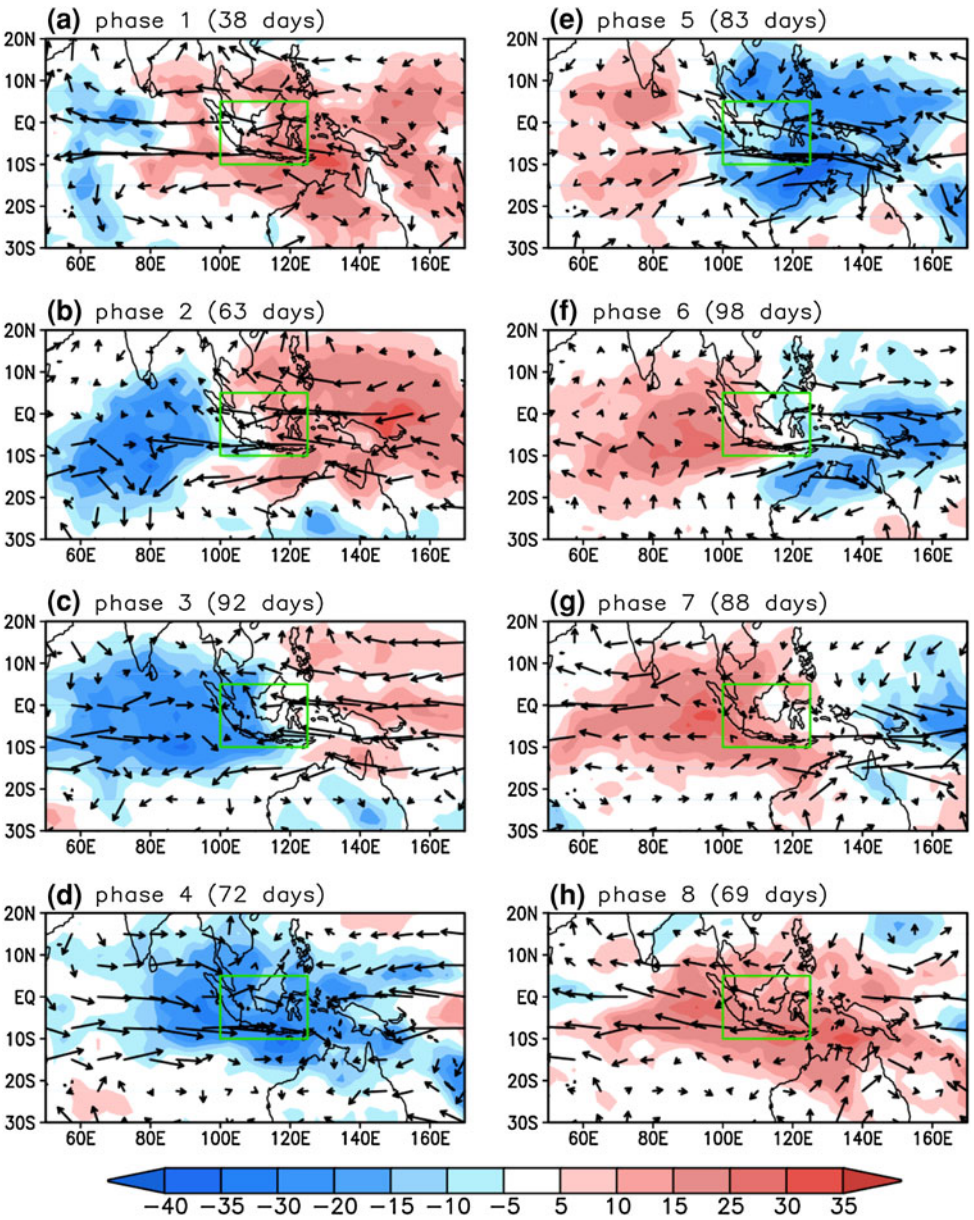

Fig. 2 Composite of OLR and 850 hPa wind anomalies for individual phases of MJO based on the RMM index. A *rectangular box* in each panel denotes the analysis domain for the present study. The number in *parentheses* denotes the number of days for each phase with the MJO amplitude greater than unity during the 10 austral summer (DJF) years (97/98–07/08)

wind anomalies in the western regime of the convective area in phase 2. During phases 3–5, convectively enhanced MJO phase passes over the Maritime Continent. Westerly wind anomalies are dominant in the analysis domain. In phases 6–8, suppressed convection penetrates the Maritime Continent followed by easterly wind anomalies. These DJF composite patterns based on the RMM index show similar evolutionary features of MJO as shown in previous studies (e.g., Wheeler and Hendon 2004).

4.3 Linkage between MJO and diurnal variation of rainfall

Figure 3a shows the PC time series of the 1st CSEOF of the TRMM rain rate, of which the loading vector was shown in Fig. 1. The mean value of the PC time series is 1.14 and its standard deviation is 1.26 exhibiting significant fluctuations of the diurnal cycle of precipitation over the study domain. The PC time series shows the modulation of the diurnal cycle of precipitation on time scales longer than 1 day; one possible source of modulation may be MJO over the western Maritime Continent. The PC time series exhibits significant power for the period of ~60 days, which is known as the periodicity of MJO (Fig. 4). This suggests that MJO exerts considerable influence on the diurnal variation of precipitation over the Maritime Continent. In order to examine the impact of MJO, the mean and the standard deviation of the PC time series were calculated as a function of the phase of MJO and are shown in Fig. 3b. The average amplitude of the seasonal cycle is

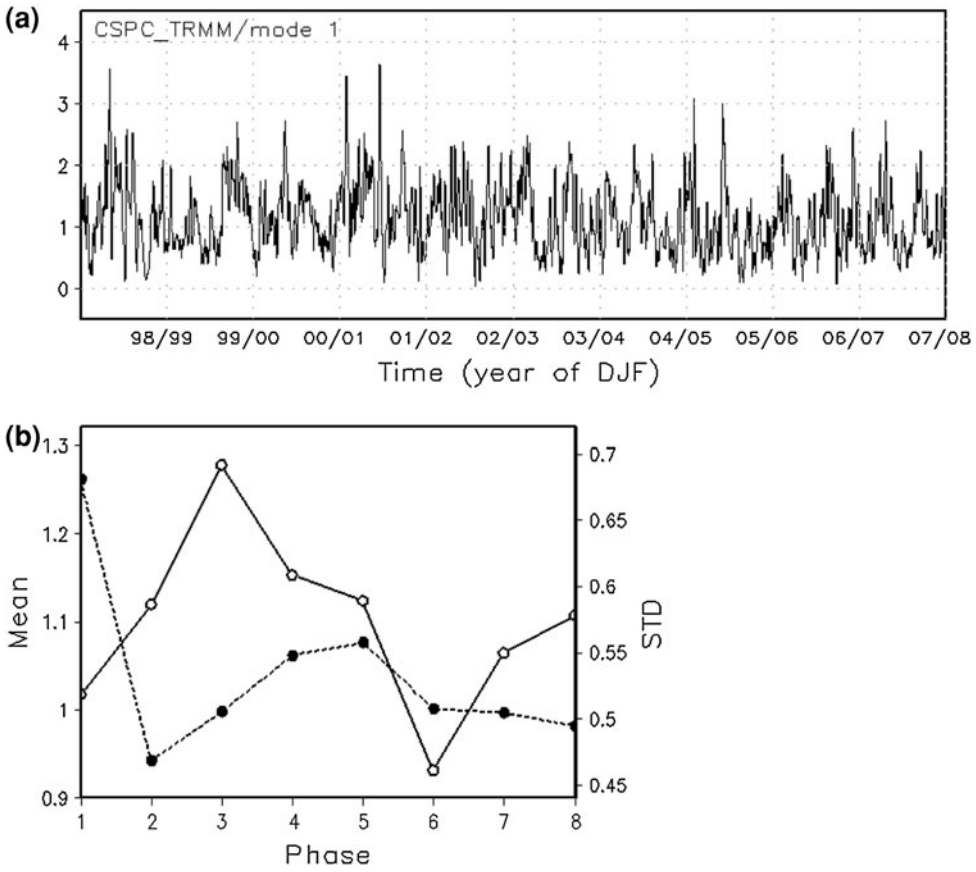

Fig. 3 **a** PC time series of the first CSEOF of the TRMM rain rate (mm h^{-1}), and **b** the mean (*solid*) and the standard deviation (*dashed*) of the PC time series for each phase of the MJO. Cases for which the MJO amplitude is less than 1 were not included in (**b**)

at its maximum during phase 3 and is at its minimum during phase 6, respectively. As shown in Fig. 2, active convection develops in phase 3 and persists until phase 5 over the Maritime Continent. In contrast, convection is suppressed over the domain during phases 6 and 7. Figure 3b suggests that the diurnal cycle of precipitation is enhanced during the active phases and is reduced during the inactive (suppressed) phases of MJO.

Among the eight MJO phases categorized by the RMM index, three phases (3, 5, and 7) of MJO are chosen to examine the physical process pertaining to the interaction between MJO and the diurnal cycle of precipitation over the western Maritime Continent. Phase 3 is considered to be not only the transition stage of convective MJO from the Indian Ocean to the western Maritime Continent also the developing stage of convection over the western Maritime Continent, and phase 5 is the mature stage of MJO in which fully developed and expanded convection is located over the Maritime Continent. On the other hand, phase 7 represents the decaying stage of convection. The domain averaged loading vector of the first CSEOF (diurnal cycle) of the rain rate for phases 3, 5, and 7 of MJO and the climatological diurnal cycle are shown in Fig. 5a. The diurnal cycle for each phase of MJO in Fig. 5 is scaled by multiplying the square root of the respective eigenvalue so

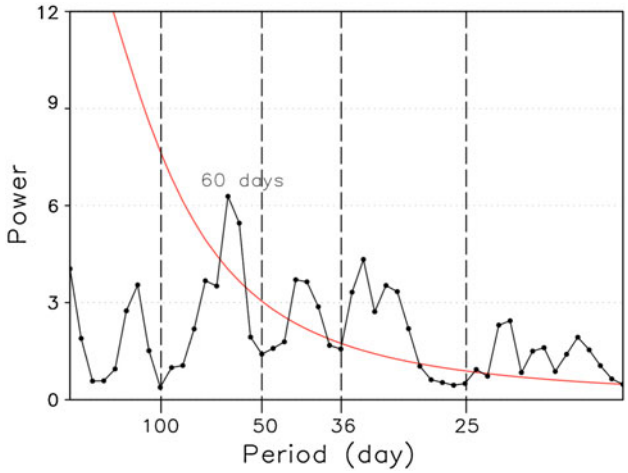

Fig. 4 Power spectrum for the PC time series of the first CSEOF shown Fig. 3a. The *red line* denotes the spectrum function of red noise with the same variance

that the magnitude of the diurnal cycle can be compared between the different phases of MJO.

The climatological diurnal cycle of the domain averaged rain rate exhibits bimodal peaks; the morning peak is associated with an increase of the rain rate over the ocean and the evening peak is related to an increase of the rain

rate over land. Consistent with Fig. 3b, the diurnal cycle during phase 3 has a greater rain rate than the climatological diurnal cycle. The magnitude of the diurnal cycle during phase 5 is larger in the morning than the climatology, however, it is smaller in the evening. The rain rate decreases markedly in phase 7.

The diurnal cycle of the rain rate for the oceanic and land areas were also computed separately. Land areas and ocean areas clearly exhibit distinct diurnal cycles of rain rate as already discussed above (Fig. 5b, c); maximum rain rate occurs in the evening (2000 LST) over land regardless of the phase of MJO whereas maximum occurs in the morning (0500 LST or 0800 LST) over the oceans. The diurnal cycle of precipitation over the seas has a smaller range compared to that over the islands.

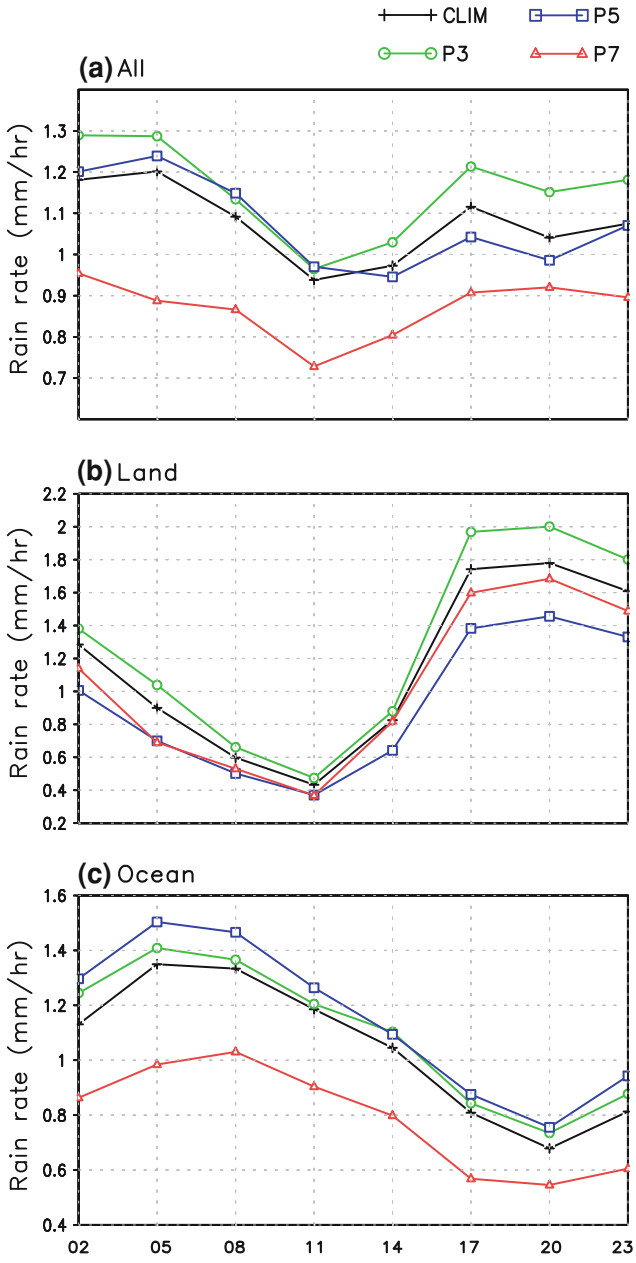

Fig. 5 Domain averaged diurnal cycle of the TRMM rain rate of climatology and for MJO phases, 3, 5, and 7: **a** for all areas, **b** for land areas, and **c** for ocean areas within the domain. The *abscissa* denotes the local standard time

As shown in Fig. 5a and discussed above, the oceanic diurnal cycle is enhanced during the active phase (phases 3 and 5) of MJO and is suppressed during the inactive phase (phase 7). Not only the magnitude but also the phase of the diurnal cycle is slightly altered with respect to the phase of MJO. During convectively active phases (phases 3 and 5) of MJO, the overall magnitude of the rain rate increases throughout the day with a peak rain rate at 0500 LST. In inactive phase (phase 7), in contrast, the rain rate reduces considerably and a peak appears at 0800 LST about 3 h later than the active phases. Since TRMM has a 3-h temporal resolution, however, it is inconclusive that the decaying phase of MJO induces a 3-h delay of rainfall peaks over the ocean. Further, rain rates at 0500 LST and 0800 LST are not significantly different. It is difficult to establish that the delay of the rainfall peak is statistically and physically significant.

On the other hand, the impact of MJO appears to be quite different over land with an increased diurnal cycle during the transition (developing) stage and a decreased diurnal cycle during the mature stage. Contrary to the oceanic case, the rain rate of the diurnal cycle records minimum values throughout the day in phase 5. During the decaying stage of MJO, the magnitude of the diurnal cycle over land is also reduced but the peak time (2000 LST) does not change.

Figure 6a shows the percentage of the oceanic region recording maximum rain rates at each local time based on the entire record. The distribution pattern is similar to the diurnal cycle of rain rate over the ocean (Fig. 5c). This is an expected result since hourly rain rate tends to increase with increase of precipitation. However, this figure denotes the regional intensity of the rain rate in each time step rather than overall rainfall amount. According to climatology, maximum rain rates are most widely observed, over 25% of the study domain, at 0800 LST. In contrast, maximum rates are observed over less than 5% of the study area at night with minimum coverage at 2000 LST. During phases 3, developing stage of MJO over the western Maritime Continent, maximum rain rates are observed more frequently at 0500 LST 3 h earlier than climatological maximum at 0800 LST. On the other hand, the spatial abundance of maximum rates is highest at 0800 LST during phases 5 and 7 as in climatology. Over land, on the other hand, the maximum rain rates are observed at 1700 LST regardless of the phase of MJO (Fig. 6b) and in climatology.

Figure 7 shows the spatial patterns of the averaged TRMM rain rates over the analysis domain in the morning (0800–1100 LST; (a), (b), (c)) and in the evening (2000–2300 LST; (d), (e), (f)). Among the eight MJO phases, 3 phases of MJO (phases 3, 5, and 7 in Fig. 5)are selected to examine the physical process pertaining to the interaction between MJO and the diurnal cycle of precipitation over the western Maritime Continent. Strong TRMM rain rates over the Java Sea and the ocean adjacent to the northwestern Borneo are evident in Fig. 7a, b. The maximum rain rate located over the Java Sea between Borneo and the Java Island in phase 3 shifts eastward in phase 5. In phase 7, or the decaying stage of MJO, rain rate prevails over the oceanic region, but their intensity is significantly reduced (Fig. 7c).

On the contrary, rain rate in the evening is mainly concentrated over islands, such as Borneo, Sumatra, and Sulawesi (Fig. 7d–f). The strongest rain rate occurs over the northwestern edge of Borneo and Sumatra in phase 3 as shown in Fig. 7d. In phase 5, the land–ocean contrast of rain rate is reduced noticeably over the Java Sea and rain rate intensity over Borneo and Sumatra also decreases. Similarly, weakened rain rates over land persist in phase 7.

4.4 How does MJO modulate the diurnal cycle?

Relevant atmospheric variables are analyzed to delineate how MJO modulates the diurnal cycle of precipitation over land and the ocean respectively. Figure 8 exhibits the 925 hPa wind speed and the streamline at 0800 LST and 2000 LST of MJO phases 3, 5, and 7 in association with the rain rate in Fig. 7. The DJF mean of the 925 hPa wind is subtracted to examine anomalies associated with MJO. The mean state is depicted in Fig. 9. The overall horizontal circulation pattern of the mean state is consistent with Fig. 2 of Johnson and Kriete (1982), which is based on the 1978–1979 International Winter Monsoon Experiment (Winter MONEX) over Southeast Asia to define the thermodynamic structure and the circulation feature of the meso-scale cloud systems and their background environment. The Maritime Continent is located downstream of the low-level northeasterly that prevails during the austral summer (Ramage 1971). In addition, westerly prevails near the equator during the wet season of the austral summer (Matsumoto 1992; Hamada et al. 2002).

MJO convection is accompanied by westerlies in the western part of the convection and easterlies in the eastern part (Zhang 2005); this feature is displayed clearly in Fig. 8. There are remarkable discrepancies in the magnitude of wind speed according to the different stages of MJO convection. In the developing stage, phase 3, convection accompanying easterlies begins to develop over the western part of the Maritime Continent. Consequently, easterlies counteract prevailing equatorial westerlies resulting in a decrease of wind speed (Fig. 8a). As convection reaches a mature stage, westerlies dominate over most of the analysis domain. Westerlies induced by MJO convection are superimposed on the monsoonal westerlies and give rise to increased wind speeds. This enhancement of the westerlies, in particular, is conspicuous primarily

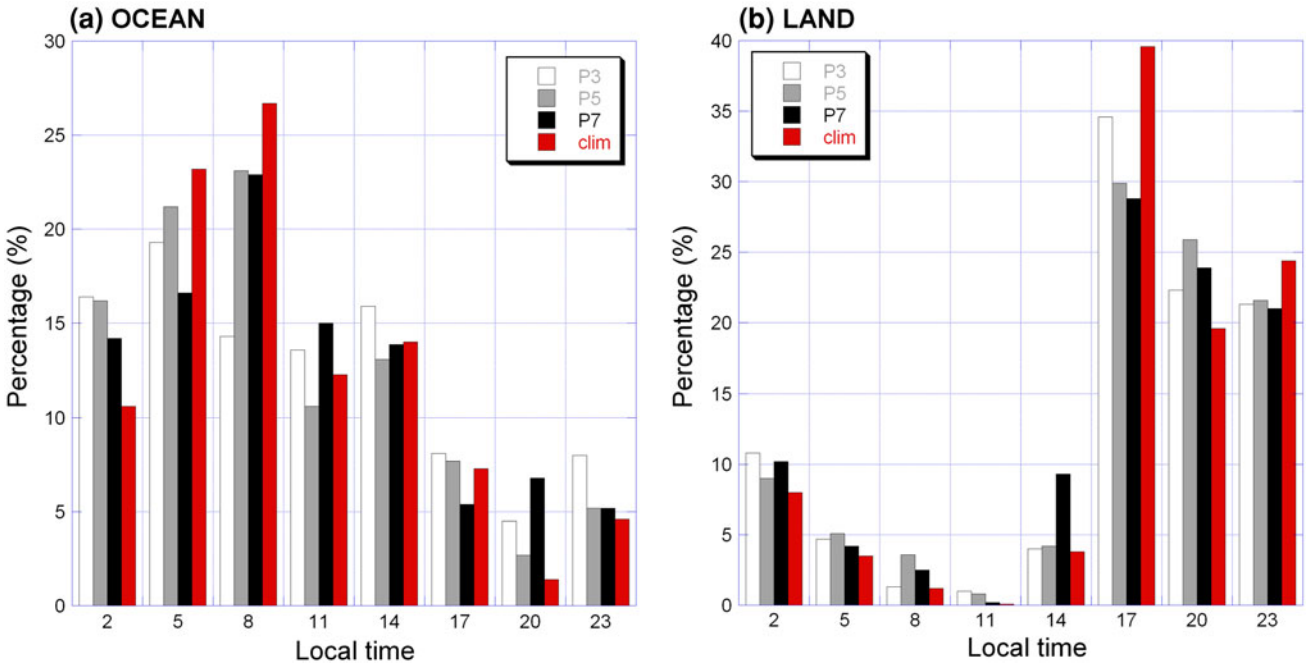

Fig. 6 Percentage of the area of **a** the ocean and of **b** land recording maximum rain rates at each local time

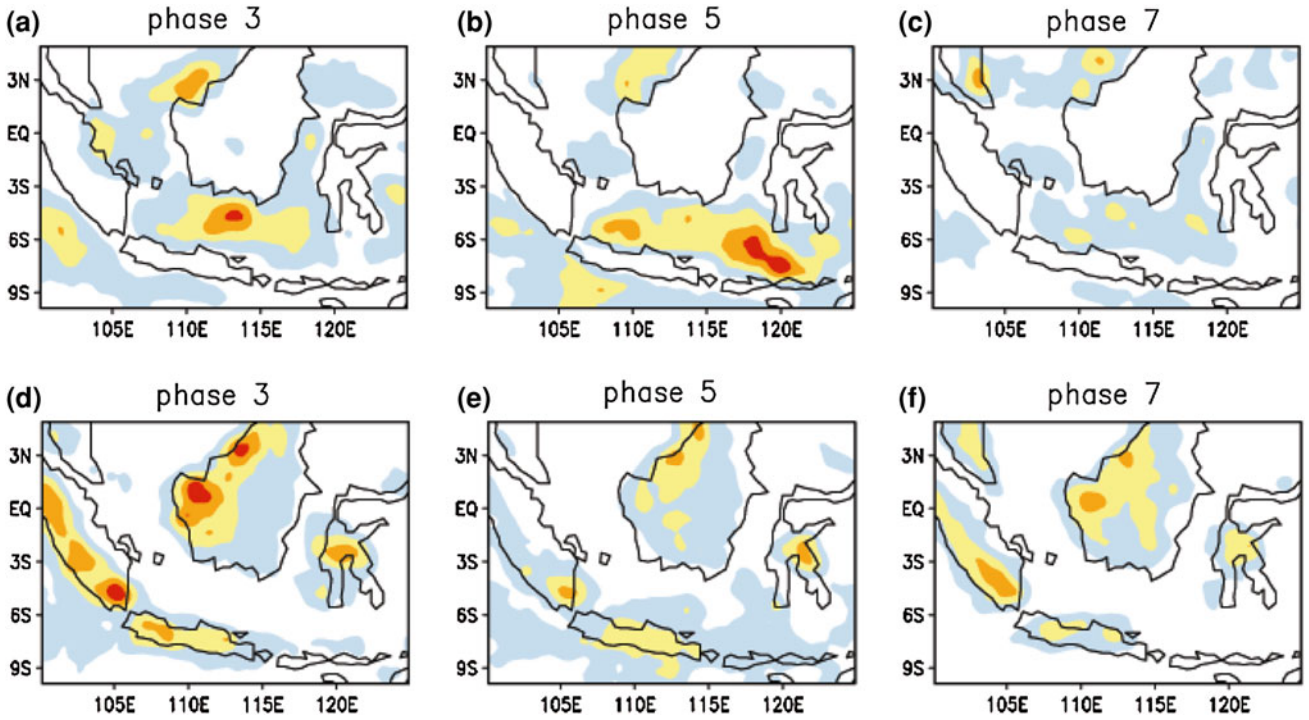

Fig. 7 Morning (0800–1100 LST) mean TRMM rain rate (mm h^{-1}) for MJO **a** phase 3, **b** phase 5, and **c** phase 7. Evening (2000–2300 LST) mean TRMM rain rate for MJO **d** phase 3, **e** phase 5, and **f** phase 7. The shading interval is 1 mm h^{-1} and the zero value is omitted

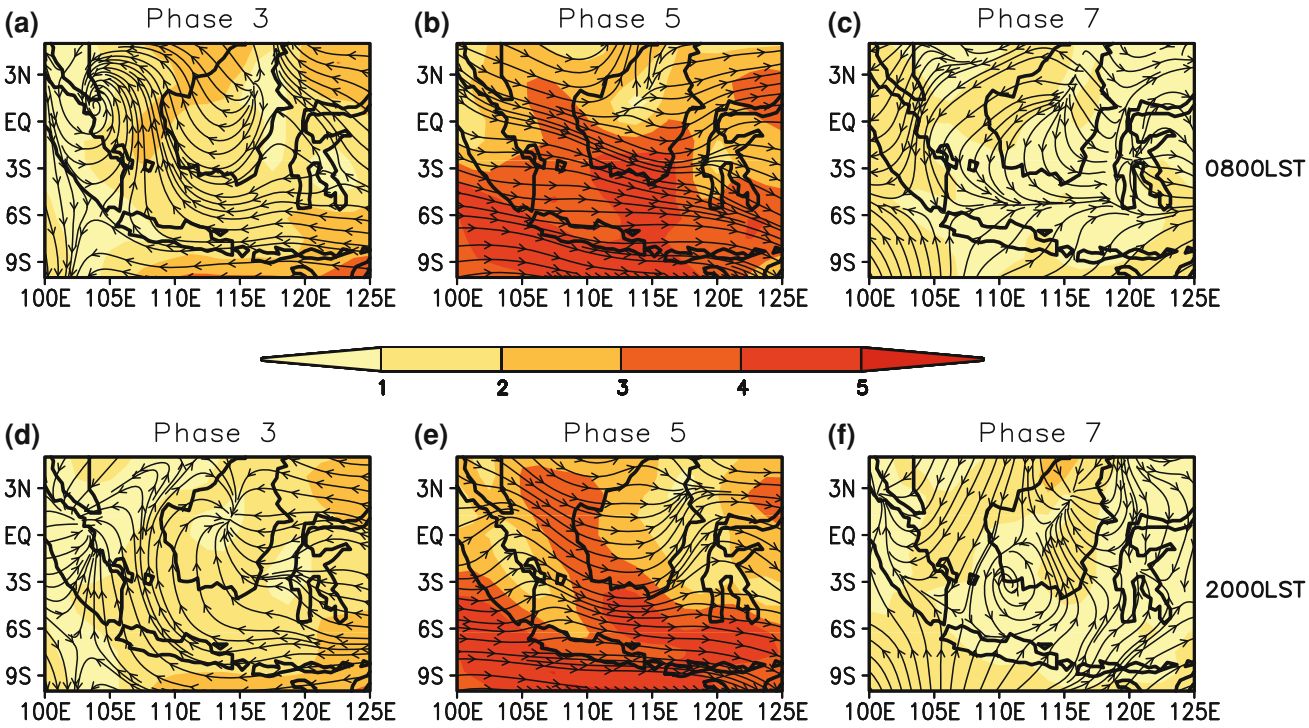

Fig. 8 Composite maps of anomalous 925 hPa wind speed (*shaded*, m s^{-1}) and streamline for MJO **a** phase 3, **b** phase 5, and **c** phase 7 at 0800 LST. **d**, **e**, **f** Are the same as **a**, **b**, **c** except at 2000 LST. Ten Austral summers (DJF) mean is subtracted before compositing

over the oceanic region specifically along the Java Sea (Fig. 8b). As noted in previous studies, topographic blocking over the Maritime Continent tends to cause surface wind to skirt around mountainous islands (Wu and Hsu 2009) and lead to the convergence of flow over the ocean. Westerly flow induced by MJO persists until phase

7 although its magnitude and spatial extent are reduced (Fig. 8c).

While horizontal flows associated with the intraseasonal disturbance are clearly depicted in Fig. 8 with respect to the MJO phases, the diurnal variation of wind generated by the land-sea breeze and mountain-valley wind over mountainous Borneo, Sumatra and adjacent oceans causes regional difference between 0800 LST and 2000 LST. While prominent converging flows are closely related to the nocturnal precipitation over Borneo at 2000 LST in phases 3 and 7, they disappear during phase 5. Strong westerlies seem to disturb the easterlies blowing from the east of Borneo and prevent the convergence over the island.

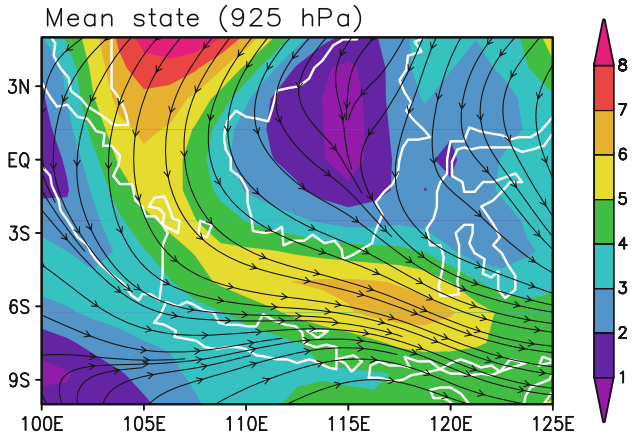

Fig. 9 The mean patterns of 925 hPa wind speed (*shaded*, m s^{-1}) and streamlines for 10 Austral summers (DJF)

Figure 10 shows divergence anomaly at 925 hPa and pressure velocity anomaly at 500 hPa. Upper panels show clear contrasts of divergence/convergence and downward/upward motion between the ocean and land at 0800 LST. Convergence along the Java Sea coincides with the upward motion at 0800 LST particularly in phase 5. Regions of convergence correspond to the areas of morning maximum precipitation over the ocean (Fig. 7a–c). Strong upward motion and low-level convergence cause heavy rainfall over the Java Sea. On the other hand, intense convergence and strong upward motion are dominant over lands in the evening (2000 LST) as shown in the lower panels. In phase 5, convergence and upward motion over Borneo, Sumatra, and Sulawesi are reduced (Fig. 10e) compared to phases 3 or 7 (Fig. 10d, f). This reduction appears to be closely linked to the weakening of the rain rate in Fig. 7e over the land areas. As mentioned above, the enhancement of the westerly flow due to MJO seems to move the location of convergence eastward.

Atmospheric instability defined by the difference of equivalent potential temperatures between 850 and 500 hPa is shown in Fig. 11 in regard to the MJO phase. Atmospheric condition becomes highly unstable during the

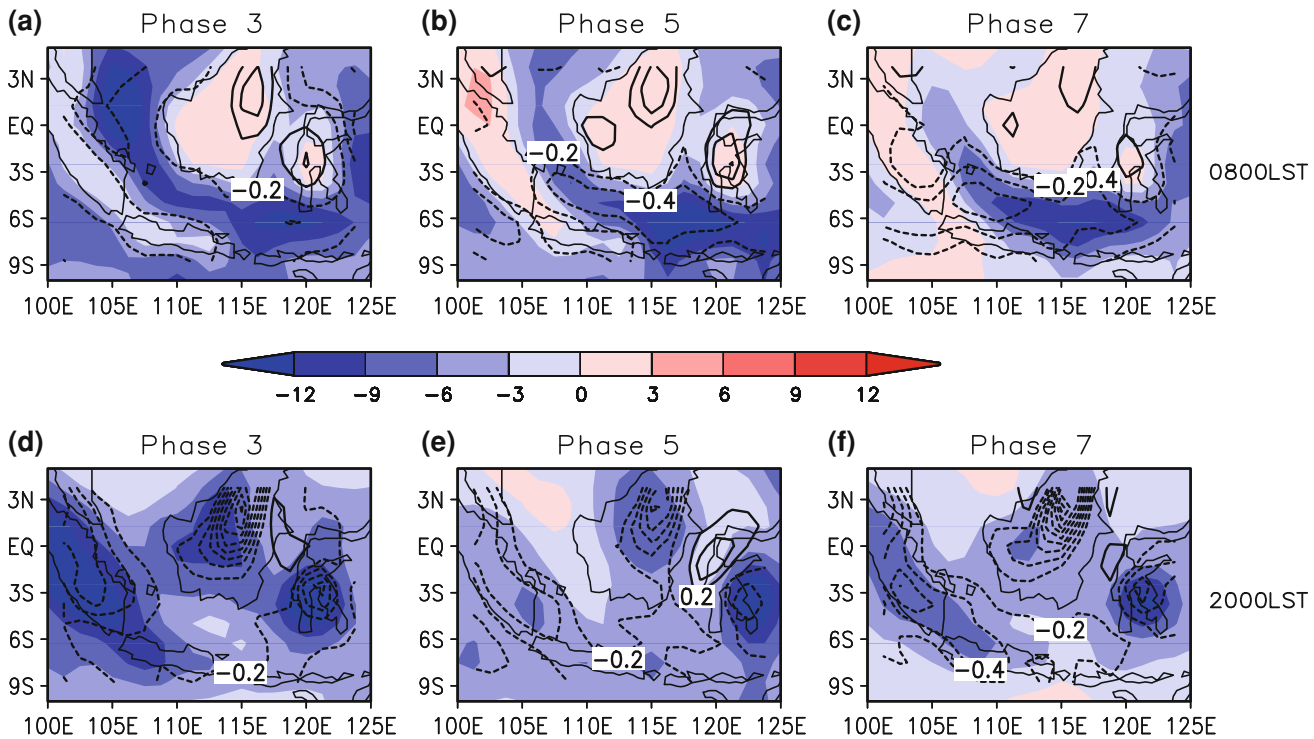

Fig. 10 Pressure velocity anomaly at 500 hPa (*shaded*, Pa s^{-1}) and divergence anomaly at 925 hPa (*contour*, 10^{-5} s^{-1}) for MJO **a** phase 3, **b** phase 5, and **c** phase 7 at 0800 LST. **d**, **e**, **f** are the same as **a**, **b**, **c** except at 2000 LST

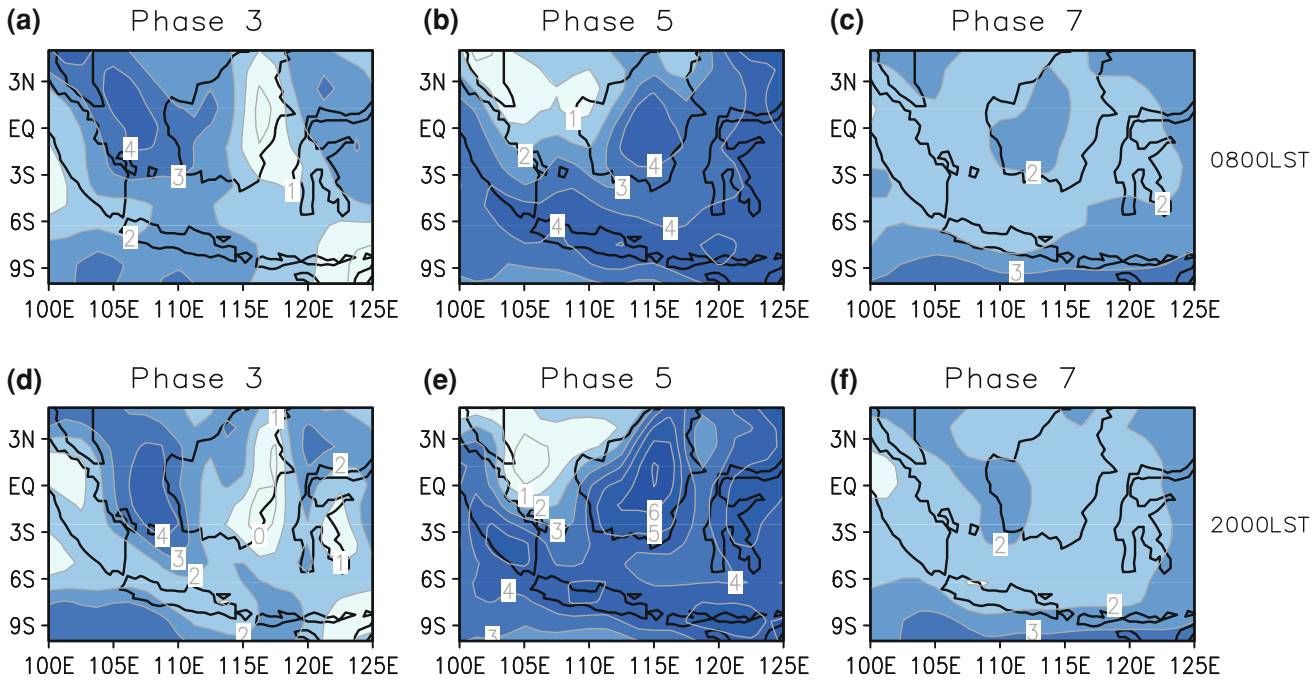

Fig. 11 Equivalent potential temperature difference between 850 hPa and 500 hPa (K) for MJO **a** phase 3, **b** phase 5, and **c** phase 7 at 0800 LST. **d**, **e**, **f** are the same as **a**, **b**, **c** except at 2000 LST

mature stage of MJO. Mountainous islands induce flow bifurcation causing near-surface winds to prevail mainly over the oceanic channels between two islands (Wu and Hsu 2009). As a result, heat flux release from the oceans to the atmosphere is enhanced by the increased surface wind leading to instability as described by the wind-induced surface heat exchange (WISHE) mechanism (Emanuel 1987; Neelin et al. 1987). Due to the weakened lower level convergence and vertical motion, strong rain rates are rarely generated, although strong convective instability is observed over Borneo in the evening during the mature stage (Fig. 11e).

Figure 12 shows the diurnal evolution of vertical motion at 500 hPa and lower level divergence at 5°S where the Java Sea is located (110°–118°E). Strong upward motion and lower level convergence is confined to the oceanic region in late evening/morning particularly during phase 5.

5 Summary and discussion

We investigate the impact of MJO on the diurnal cycle of rainfall over the western Maritime Continent by applying CSEOF analysis to the TRMM rain rate and JRA-25 reanalysis data. The RMM index designed by Wheeler and Hendon (2004) is adopted to define the intensity and phase of MJO. Based on the PC time series of the diurnal cycle of rain rates, MJO with intraseasonal time scales is found to modulate the diurnal variation of rainfall over the analysis domain. In addition, during the active phases of MJO as defined by the RMM index, the average magnitude of the PC time series tends to increase indicating an enhancement of the diurnal cycle.

CSEOF analysis is also performed separately for each MJO phase as defined by the RMM index. We demonstrate that domain averaged hourly maximum rain rate tends to increase when the convectively active phase of MJO approaches and resides over the Maritime Continent (phase 3). In contrast, when convectively inactive MJO phase is found over the region (phase 7), hourly maximum rain rate tends to subside. The magnitude of the diurnal cycle in the morning is larger than the magnitude of climatology, but is smaller in the evening during the mature phase (phase 5). The rain rate change due to MJO differs over the ocean and land. This discrepancy is most apparent during phase 5. While diurnally varying oceanic rain rates record maximum values, terrestrial rain rates show minimum values throughout the day during phase 5. Precipitation becomes more intense over the Java Sea in the morning and weakens over Borneo and Sumatra in the evening during phase 5.

The percentage of the oceanic region recording maximum rain rates at each local time is examined with respect to the MJO phase. During the developing stage of MJO convection over the western Maritime Continent (phases 3–4), the percentage is greatest at 0500 LST unlike the climatology and other phases for which the percentage reaches its maximum at 0800 LST. Over land, in contrast, maximum rain rates are observed at 1700 LST regardless

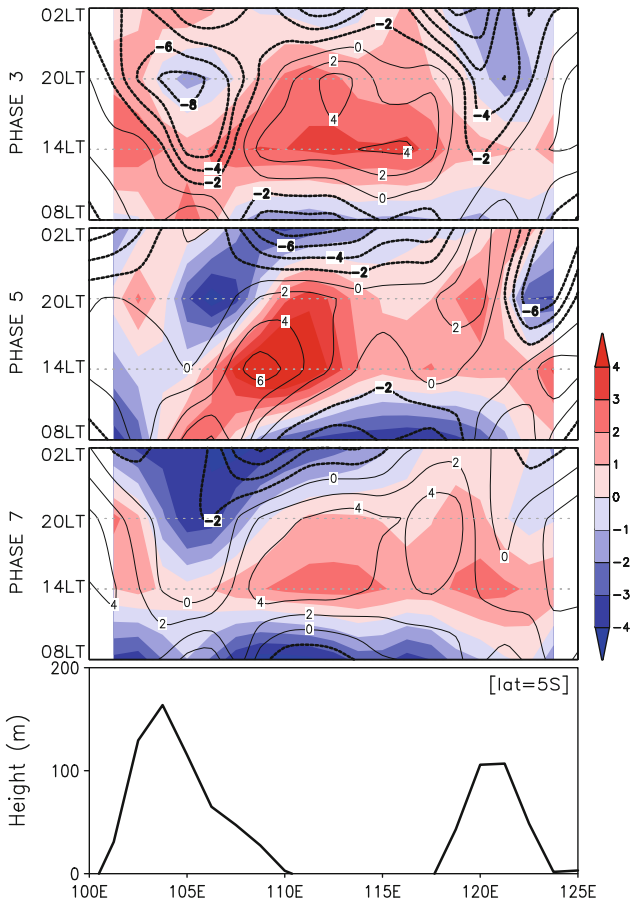

Fig. 12 Time-longitude plots of pressure velocity at 500 hPa (*shaded*, Pa s^{-1}) and divergence at 925 hPa (*contour*, 10^{-5} s^{-1}) at 5°S for MJO **a** phase 3, **b** phase 5, and **c** phase 7. Vertical velocity was multiplied by 100. Land terrain is described at the *bottom panel*

of the MJO phase. We hypothesize that the 3-h advance of the maximum rain rates over the oceans during phases 3 and 4 is tied to the combined effect of the physical process of the diurnal cycle of precipitation over the open ocean, which is not fully understood, and the initiation and propagation mechanisms of MJO. This combined effect leads to favorable conditions for precipitation earlier over oceanic regions. However, verifying this relationship requires further detailed examination.

Our results suggest that the anomalous low-level winds accompanied by MJO interact with the monsoonal flow over the Maritime Continent. Prevailing westerlies to the west of the convective MJO in phase 5 are superimposed on monsoonal westerlies over the equator and increase wind speed mainly over the Java Sea due to the blocking effect of orography. Mountainous islands induce flow bifurcation making near-surface winds prevail over the oceanic channels between two islands (Wu and Hsu 2009). As a result, heat flux release from the oceans to the atmosphere is enhanced by the increased surface wind giving rise to instability as described in the wind-induced surface heat exchange (WISHE) mechanism (Emanuel 1987; Neelin et al. 1987). This may contribute to heavy rainfall over the Java Sea in the morning during phase 5.

The presence of strong convergence at 925 hPa in conjunction with an upward motion at 500 hPa over the Java Sea also explains strong rain rate in the morning during phase 5. On the other hand, evening convergence and vertical velocity over the islands tends to be weaker during the mature phase (phase 5) than the developing or decaying phases (phases 3 or 7). Strong westerlies contributed by the anomalous wind accompanying MJO and the seasonal flow during phase 5 tend to interrupt convergence over islands, which plays an important role in inducing nighttime rainfall. This interruption results in decreased rain rate over the terrestrial regions compared to phases 3 and 7. The existence of fully developed cloud clusters of MJO over the Maritime Continent may also contribute to decreased rain rate over the islands. As cloud clusters reside over the Maritime Continent during phase 5, they intercept daytime solar radiation, which results in decreased pressure gradient between land and the ocean. Ultimately, the decreased pressure gradient leads to a decreased precipitation over land in the afternoon. This hypothesis should be examined further using cloud data.

We investigated the impact of MJO on the diurnal cycle of rainfall over the Maritime Continent, and attempted to explain the physical processes behind the land/ocean differential impacts of MJO on the diurnal variation of precipitation. Large regional variability is inherent in the diurnal cycle (Lim and Seo 2000) and it cannot be ruled out that inhomogeneous surface condition over the Maritime Continent is responsible for differential impact of MJO (Byon and Lim 2005). Moreover, dynamical link between the diurnal cycle and MJO competing for the limited source of moisture may involve multiple interactions of complicated physical mechanisms. Sophisticated analysis based on dense observations and numerical modeling is needed to answer these questions.

Acknowledgments This work was funded by the Korea Meteorological Administration Research and Development Program under Grant CATER 2006-2201. J.-H. Oh and G.-H. Lim were supported by the second stage of the Brain Korea 21 Project.

References

Bowman K, Collier J, North G, Wu Q, Ha E, Hardin J (2005) Diurnal cycle of tropical precipitation in tropical rainfall measuring mission (TRMM) satellite and ocean buoy rain gauge data. J Geophys Res. doi:10.1029/2005JD005763

Byon J, Lim G (2005) Diurnal variation of tropical convection during TOGA COARE IOP. Adv Atmos Sci 22:685–702

Chen S, Houze Jr R (1997) Diurnal variation and life-cycle of deep convective systems over the tropical Pacific warm pool. Q J R Meteorol Soc 123(538):357–388

Dayem K, Noone D, Molnar P (2007) Tropical western Pacific warm pool and maritime continent precipitation rates and their contrasting relationships with the Walker Circulation. J Geophys Res 112. doi:10.1029/2006JD007870

Emanuel K (1987) An air-sea interaction model of intraseasonal oscillations in the tropics. J Atmos Sci 44:2324–2340

Hall J, Matthews A, Karoly D (2001) The modulation of tropical cyclone activity in the Australian region by the Madden-Julian oscillation. Mon Weather Rev 129:2970–2982

Hamada J, Yamanaka M, Matsumoto J, Fukao S, Winarso P, Sribimawati T (2002) Spatial and temporal variations of the rainy season over Indonesia and their link to ENSO. J Meteorol Soc Jpn 80:285–310

Hendon H, Liebmann B (1990) The Intraseasonal (30–50 day) Oscillation of the Australian summer monsoon. J Atmos Sci 47:2909–2924

Hendon H, Salby M (1994) The life cycle of the Madden-Julian oscillation. J Atmos Sci 51:2225–2237

Houze R Jr, Geotis S, Marks F Jr, West A (1981) Winter monsoon convection in the vicinity of North Borneo. Part I: structure and time variation of the clouds and precipitation. Mon Weather Rev 109:1595–1614

Hsu H, Lee M (2005) Topographic effects on the eastward propagation and initiation of the Madden-Julian oscillation. J Clim 18:795–809

Huffman G, Adler R, Bolvin D, Gu G, Nelkin E, Bowman K, Hong Y, Stocker E, Wolff D (2007) The TRMM multisatellite precipitation analysis (TMPA): Quasi-global, multiyear, combined-sensor precipitation estimates at fine scales. J Hydro 8:38–55

Ichikawa H, Yasunari T (2006) Time-space characteristics of diurnal rainfall over Borneo and surrounding oceans as observed by TRMM-PR. J Clim 19:1238–1260

Ichikawa H, Yasunari T (2007) Propagating diurnal disturbances embedded in the Madden-Julian Oscillation. Geophys Res Lett 34. doi:10.1029/2007GL030480

Ichikawa H, Yasunari T (2008) Intraseasonal variability in diurnal rainfall over New Guinea and the surrounding oceans during austral summer. J Clim 21:2852–2868

Johnson R, Kriete D (1982) Thermodynamic and circulation characteristics, of winter monsoon tropical mesoscale convection. Mon Weather Rev 110:1898–1911

Kessler W, Kleeman R (2000) Rectification of the Madden-Julian oscillation into the ENSO cycle. J Clim 13:3560–3575

Kim K, North G (1997) EOFs of harmonizable cyclostationary processes. J Atmos Sci 54:2416–2427

Kim K, North G, Huang J (1996) EOFs of one-dimensional cyclostationary time series: computations, examples, and stochastic modeling. J Atmos Sci 53:1007–1017

Lawrence D, Webster P (2002) The boreal summer intraseasonal oscillation: relationship between northward and eastward movement of convection. J Atmos Sci 59:1593–1606

Liberti G, Cheruy F, Desbois M (2001) Land effect on the diurnal cycle of clouds over the TOGA COARE area, as observed from GMS IR data. Mon Weather Rev 129:1500–1517

Lim G, Seo A (2000) Diurnal and semidiurnal variations in the time series of 3-hourly assimilated precipitation by NASA GEOS-1. J Clim 16:2923–2940

Maloney E, Hartmann D (2000) Modulation of eastern North Pacific hurricanes by the Madden-Julian oscillation. J Clim 13:1451–1460

Matsumoto J (1992) The seasonal changes in Asian and Australian monsoon regions. J Meteor Soc Jpn 70:257–273

Mori S, Jun-Ichi H, Tauhid Y, Yamanaka M, Okamoto N, Murata F, Sakurai N, Hashiguchi H, Sribimawati T (2004) Diurnal land-sea rainfall peak migration over Sumatera Island, Indonesian Maritime Continent, observed by TRMM satellite and intensive rawinsonde soundings. Mon Weather Rev 132:2021–2039

Neelin J, Held I, Cook K (1987) Evaporation-wind feedback and low-frequency variability in the tropical atmosphere. J Atmos Sci 44:2341–2348

Nesbitt S, Zipser E (2003) The diurnal cycle of rainfall and convective intensity according to three years of TRMM measurements. J Clim 16:1456–1475

Onogi K, Tsutsui J, Koide H, Sakamoto M, Kobayashi S, Hatsushika H, Matsumoto T, Yamazaki N, Kamahori H, Takahashi K, Kadokura S, Wada K, Kato K, Oyama R, Ose T, Mannoji N, Taira R (2007) The JRA-25 reanalysis. J Meteor Soc Jpn 85:369–432

Qian J (2008) Why precipitation is mostly concentrated over islands in the maritime continent. J Atmos Sci 65:1428–1441

Ramage C (1971) Monsoon meteorology. Academic Press, New York, p 295

Rui H, Wang B (1990) Development characteristics and dynamic structure of tropical intraseasonal convection anomalies. J Atmos Sci 47:357–379

Seo K, Kim K (2003) Propagation and initiation mechanisms of the Madden-Julian oscillation. J Geophys Res 108:4384. doi:10.1029/2002JD002876

Slingo J, Sperber K, Boyle J, Ceron J, Dix M, Dugas B, Ebisuzaki W, Fyfe J, Gregory D, Gueremy J (1996) Intraseasonal oscillations in 15 atmospheric general circulation models: results from an AMIP diagnostic subproject. Clim Dyn 12:325–357

Sperber K (2003) Propagation and the vertical structure of the Madden-Julian oscillation. Mon Weather Rev 131:3018–3037

Sui C, Lau K (1992) Multiscale phenomena in the tropical atmosphere over the western Pacific. Mon Weather Rev 120:407–430

Tian B, Waliser D, Fetzer E (2006) Modulation of the diurnal cycle of tropical deep convective clouds by the MJO. Geophys Res Lett 33. doi:10.1029/2006GL027752

Wheeler M, Hendon H (2004) An all-season real-time multivariate MJO index: development of an index for monitoring and prediction. Mon Weather Rev 132:1917–1932

Wu C, Hsu H (2009) Topographic influence on the MJO in the maritime continent. J Clim 22:5433–5448

Yang G, Slingo J (2001) The diurnal cycle in the tropics. Mon Weather Rev 129:784–801

Yang S, Smith E (2006) Mechanisms for diurnal variability of global tropical rainfall observed from TRMM. J Clim 19:5190–5226

Zhang C (2005) Madden-Julian oscillation. Rev Geophys 43:RG2003. doi:10.1029/2004RG000158

Zhang C, Gottschalck J (2002) SST anomalies of ENSO and the Madden-Julian oscillation in the Equatorial Pacific. J Clim 15:2429–2445

Zhou L, Wang Y (2006) Tropical rainfall measuring mission observation and regional model study of precipitation diurnal cycle in the New Guinean region. J Geophys Res 111. doi:10.1029/2006JD007243